Dalton Transactions

Cite this: *Dalton Trans.*, 2011, **40**, 10897

www.rsc.org/dalton

PAPER

Density functional studies on dinuclear $\{Ni^{II}Gd^{III}\}$ and trinuclear $\{Ni^{II}Gd^{III}Ni^{II}\}$ complexes: magnetic exchange and magneto-structural maps†

Saurabh Kumar Singh, Neeraj Kumar Tibrewal and Gopalan Rajaraman*

Received 8th April 2011, Accepted 27th June 2011
DOI: 10.1039/c1dt10600g

Theoretical calculations using density functional methods have been performed on two dinuclear $\{Ni^{II}–Gd^{III}\}$ and two trinuclear $\{Ni^{II}–Gd^{III}–Ni^{II}\}$ complexes having two and three μ-OR (R = alkyl or aromatic groups) bridging groups. The different magnetic behaviour, having moderately strong ferromagnetic coupling for complexes having two μ-OR groups and weak ferromagnetic coupling for complexes having three μ-OR groups, observed experimentally is very well reproduced by the calculations. Additionally, computation of overlap integrals MO and NBO analysis reveals a clear increase in antiferromagnetic contribution to the net exchange for three μ-OR bridged {Ni–Gd} dimers and also provides several important clues regarding the mechanism of magnetic coupling. Besides, MO and NBO analysis discloses the role of the empty 5d orbitals of the Gd^{III} ion on the mechanism of magnetic coupling. Magneto-structural correlations for Ni–O–Gd bond angles, Ni–O and Gd–O bond distances, and the Ni–O–Gd–O dihedral angle have been developed and compared with the published experimental {Ni–Gd} structures and their *J* values indicate that the Ni–O–Gd bond angles play a prominent role in these types of complexes. The computation has then been extended to two trinuclear $\{Ni^{II}–Gd^{III}–Ni^{II}\}$ complexes and here both the {Ni–Gd} and the {Ni–Ni} interactions have been computed. Our calculations reveal that, for both structures studied, the two {NiGd} interactions are ferromagnetic and are similar in strength. The {Ni–Ni} interaction is antiferromagnetic in nature and our study reveals that its inclusion in fitting the magnetic data is necessary to obtain a reliable set of spin Hamiltonian parameters. Extensive magneto-structural correlations have been developed for the trinuclear complexes and the observed *J* trend for the trinuclear complex is similar to that of the dinuclear {Ni–Gd} complex. In addition to the structural parameters discussed above, for trinuclear complexes the twist angle between the two Ni–O–Gd planes is also an important parameter which influences the *J* values.

1. Introduction

Molecules which retain magnetisation in the absence of magnetic field are called single molecule magnets (SMMs).[1] They have wide spread potential applications – ranging from high-density information storage devices to solid-state Q-bits in quantum computing.[2,3] Enhancing the barrier height (related to the spin ground state *S* and axial zero-field splitting *D*) for the reorientation of magnetisation in SMMs remains one of the primary challenges in taking these SMMs to end-user applications. During the last decade, hundreds of SMMs containing transition metal atoms have been reported, notably a $\{Mn_6^{III}\}$ SMM with a barrier height of 86 K – the largest for any transition metal SMMs known to-date.[4]

An alternative strategy to increase the barrier height emerges from a simple idea of employing highly anisotropic ions such as lanthanides in the cluster aggregation.[5] With lanthanides, even simple mononuclear Tb^{III}/Dy^{III} complexes are reported to have SMM characteristics with a large energy barrier for relaxation of magnetisation.[6–9] A recent report of a $\{Dy_4^{III}\}$ cluster with a record barrier height of 170 K illustrates the importance of 4f ions in the cluster aggregation.[10] A particular problem associated with clusters containing only 4f elements are the very weak exchange interactions and fast quantum tunnelling of the magnetisation leading to the isolation of SMMs with a large barrier height, a challenging task. To overcome this drawback, 3d metal ions are combined with 4f ions to make {3d–4f}[5] clusters and this strategy had produced several novel SMMs

Department of Chemistry, Indian Institute of Technology Bombay, Powai, Mumbai, 400076, India. E-mail: rajaraman@chem.iitb.ac.in; Fax: (+91)22-2576-7152; Tel: (+91)-22-2576-7183

† Electronic supplementary information (ESI) available: DFT computed energies, structures of all model complexes, computed overlap integrals, and spin densities of important atoms, correlation developed by varying Ni–Ni distance in model **1b**, magneto-structural correlations developed for complex **2**, simulation of the susceptibility behaviour for complex **3**, NBO analysis data and list of other Ni–Gd di and trinuclear complexes reported with their selected structural parameters and experimental *J* values. See DOI: 10.1039/c1dt10600g

with attractive blocking temperatures.[11–21] Apart from SMM characteristics, other applications for the {3d–4f} complexes, such as magnetic refrigerants, has been suggested.[22]

The synthesis of a new generation SMMs requires a thorough understanding and control of the microscopic spin Hamiltonian parameters. In this regard, computational tools are indispensable – both in calculating the spin Hamiltonian parameters as well as in predicting the magnetic properties of the paramagnetic complexes.[23–27] Despite extensive experimental studies on {3d–4f} systems, there are only a few reports on theoretical side[28–31] particularly on the evaluation of magnetic exchange interaction J and in understanding the mechanism of magnetic coupling.

Based on the experimental data, many qualitative mechanisms for the {3d–4f} coupling have been put forth. It is common knowledge that the 4f electrons of the lanthanides are effectively shielded and their interaction with ligands and 3d orbitals are negligible. Initially, to explain the magnetic coupling in {3d–4f} complexes, a charge transfer mechanism is invoked where a partial charge transfer from the 3d orbitals of the metal ions to the empty 6 s orbitals of the Gd^{III} atom was proposed.[32–35] Later, an alternative mechanism using empty 5d orbitals of the Gd^{III} instead of the 6 s orbitals was suggested.[36–38] An *ab initio* CASSCF/PT2 study on a {Cu–Gd}[39] dimer to understand the mechanism of coupling provides several useful hints, especially revealing the importance of the 5d orbitals in the mechanism of magnetic coupling.[40]

Recently, comprehensive DFT studies on {Cu–Gd} dinuclear complexes have been performed by us[31] and others[41] with an aim to establish a computational protocol to calculate the J values, to comprehend the mechanism of coupling and to develop magneto-structural correlations. These studies also support the vital role of the 5d orbitals in the coupling mechanism. Although the {Cu–Gd} pair is the simplest {3d–4f} pair which can be treated easily with sophisticated theoretical methods, they are not ideal candidates for SMMs as both metal ions do not inherit any large anisotropy in their ground state. On the other hand, replacing Cu^{II} by Ni^{II} ions yields a {Ni–Gd}[44,45] pair, which is an appealing candidate for SMMs as Ni^{II} ions generally exhibit large anisotropy. For example, recently some mononuclear Ni^{II} complexes have been reported to have a very large negative axial zero-field splitting (D = –7.7 cm^{-1}) parameter.[46] Over the years many dinuclear and polynuclear {Ni–Ln} complexes have been reported, some of which possess SMM characteristics.[18,44–48] The nature of the {Ni–Gd} interaction is also intriguing among the structures reported as it varies from moderately ferromagnetic[49] to weakly antiferromagnetic.[51] In polynuclear complexes, in addition to the near-neighbour {Ni–Gd} interactions, the next-nearest-neighbour {Ni–Ni} interactions also play a pivotal role in determining the ground state as in some structures they compete with the {Ni–Gd} interaction.[48,50]

Here we have chosen to focus our attention on two dinuclear {Ni–Gd}[18,19] and two trinuclear {Ni–Gd–Ni}[40] complexes. We have computed the magnetic exchange interactions for all four complexes. For trinuclear complexes we have computed both near-neighbour {Ni–Gd} and next-nearest-neighbour {Ni–Ni} interactions. Besides, calculations have been performed on several fictitious model complexes and MO and NBO analysis has been performed to shed light on the mechanism of coupling. Finally, we have developed extensive magneto-structural correlations for both the dinuclear {Ni–Gd} and the trinuclear {Ni–Gd–Ni} complexes.

2. Computational details

In dinuclear complexes, the magnetic exchange interaction between Ni^{II} and Gd^{III} ions is described by the following spin-Hamiltonian:

$$\hat{H} = -J\,\hat{S}_{Gd}\hat{S}_{Ni}$$

were J is the isotropic exchange coupling constant and S_{Gd} and S_{Ni} are spins on Gd^{III} ($S = 7/2$) and Ni^{II} ($S = 1$) atoms respectively. The DFT calculations combined with the broken symmetry (BS) approach[52] has been employed to compute the J values.

The BS method has a proven record of yielding good numerical estimated of J constants for a variety of complexes.[23,26,53,54] A detailed technical discussion on computational details on the evaluation of J values using the broken symmetry approach on dinuclear as well as trinuclear complexes can be found elsewhere.[25,54] Here, we have performed most of our calculations using the Gaussian 03 suite of programs.[55] We have employed a hybrid B3LYP functional[56] along with a double-zeta quality basis set employing Cundari–Stevens (CS) relativistic effective core potential on Gd atoms[57] and LanL2DZ ECP basis set on Ni[58] with an all electron 6-31G basis set[59] for the rest of the atoms (*level I*). A comprehensive method assessment performed earlier on {Cu–Gd} complexes by us reveals that this combination yields a good estimate of the J constants.[31] Since these calculations have great difficulty in SCF convergence, the Jaguar suite of programs[60] has been employed to generate the initial guess which is then transferred to Gaussian for the SCF iterations. We have also performed all electron calculations for comparison using the ORCA suite of programs,[61] employing Nakajima and co-workers all electron basis set on Gd,[62] Ahlrichs and co-workers TZVP on Ni,[63] along with their SVP basis set on the rest of the elements. These calculations have been performed by incorporating relativistic effects *via* the Douglas–Kroll–Hess method[64,65] (*level II*). A very tight SCF convergence has been employed throughout.

For trinuclear complexes the following spin Hamiltonian has been adopted:

$$\hat{H} = -J_1\hat{S}_{Ni_A}\hat{S}_{Gd} - J_2\hat{S}_{Gd}\hat{S}_{Ni_B} - J_3\hat{S}_{Ni_A}\hat{S}_{Ni_B}$$

The magnetic exchange interactions in trinuclear complexes were extracted using the pair-wise interaction model,[23] where four spin configurations are computed to extract three different exchange interactions J_1–J_3. The following four spin configurations have been computed (i) all spin up (S = 11/2), (ii) spin down on only Ni_A ($S = 7/2$), (See Fig. 1c for labelling) (iii) spin down on only Ni_B ($S = 7/2$) (iv) spin down on both Ni_A and Ni_B ($S = 3/2$). The energy differences between the spin configurations are equated to the corresponding exchange interactions from which all three J values have been extracted.[23]

3. Results and discussion

The majority of the reported {Ni–Gd} complexes possess either two or three μ-OR (R = alkyl or aromatic groups) bridging groups which mediate the exchange interaction between the two metals. Some higher nuclearity complexes have additional carboxylate bridges.[50,66,67] Among several dinuclear {Ni–Gd} and trinuclear {Ni–Gd–Ni} complexes reported, two classes of compounds

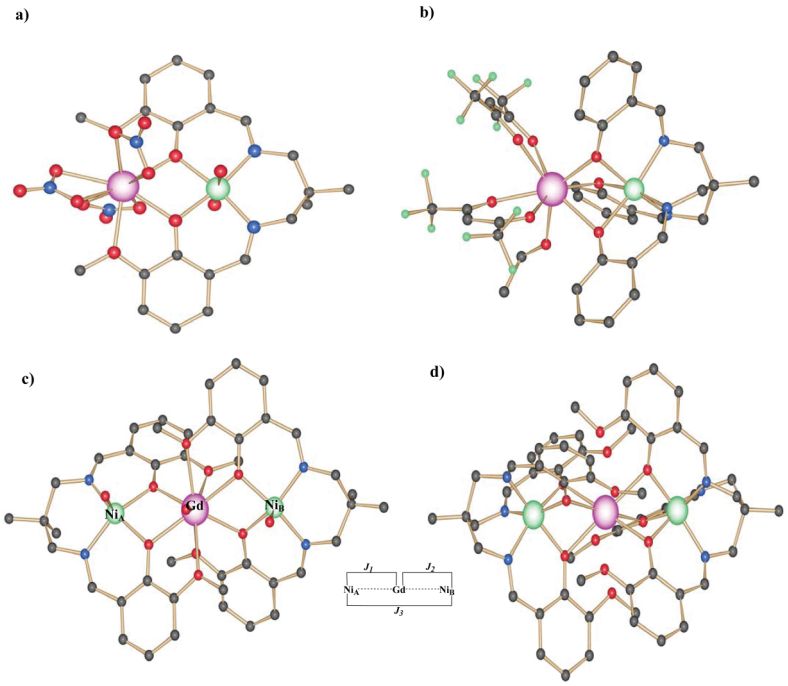

Fig. 1 Crystal structures of complexes a) **1** b) **2** c) **3** and d) **4** together with the exchange topology adopted for trinuclear complexes **3** and **4**.

distinctly emerge and they are categorised as *type I* and *II* as shown in Scheme 1.

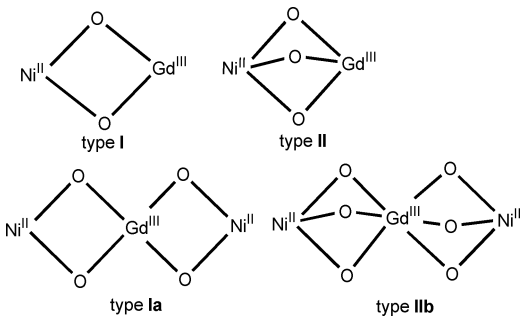

Scheme 1

The four structural motifs shown in Scheme 1 are the basic building blocks of several polynuclear {Ni–Gd} complexes and therefore here we have decided to focus our attention on these structures.

3.1 Exchange interaction in dinuclear {Ni–Gd} complexes

Here we have employed DFT calculations on the full structure of $[L^1Ni(H_2O)_2Gd(NO_3)_3]$ (**1**) (L^1 = [2,2′-[2,2-Dimethyl-1,3-propanediylbis(nitrilomethylidyne)]bis(6-methoxyphenolato)(2-)] nickel(II)]) (see Fig. 1) and $[(NiL^2)Gd(hfac)_2(EtOH)]$ (**2**) (H_3L^2 = 1,1,1-tris(*N*-salicylideneaminomethyl)ethane and Hhfac = hexafluoroacetylacetone) to compute the magnetic exchange between the two metal atoms. Complexes **1** and **2** belong to structural core *type* I and II respectively. Apart from the number of bridges present, the structural differences which are expected to affect the magnetic coupling between the two metal atoms are Ni–O and Gd–O distances, Ni–O–Gd angles and the Ni–O–Gd–O dihedral angle. Selected structural parameters of complex **1** and **2** are collected in Table 1. The inter-metallic Ni–Gd distance is 3.522 Å in complex **1** compared to 3.169 Å in **2**. The average Ni–O bond lengths and average Ni–O–Gd angles are ~0.05 Å and 16.4° longer/larger in **2** compared to that of complex **1** (See Table 1). Additionally, the Ni–O–Gd–O dihedral angles are 2.4° *vs.* 38.4°, 38.9° and 34.6° for complex **1** and **2** respectively.

The experimental magnetic susceptibility studies yield a ferromagnetic exchange between Ni^{II} and Gd^{III} ions in both cases, with the J values of +3.6 cm^{-1} for **1** and +0.34 cm^{-1} for **2**. The DFT calculated J values for complexes **1** and **2** using theoretical *level I* and *II* are listed in Table 2 (the computed total energies together with the $<S^2>$ values of the complexes and their models are listed in Table S1 and S2, ESI†). In general there is a good agreement between the experimental and theoretical values, with the J calculated using *level I* being slightly superior to that of *level II*. Our previous method assessment calculations on the {Cu–Gd} dimer reveal similar conclusions.[31]

3.2 Mechanism of magnetic coupling

The {Ni–Gd} interaction is in general ferromagnetic in nature with a very few exceptions.[51] Both complexes **1** and **2** (also the complexes **3** and **4** see later) exhibit ferromagnetic {Ni–Gd} interactions. Between complexes **1** and **2**, the J value of **1** is larger than **2**. In general, *type I* structures exhibit a larger ferromagnetic J compared to that of the *type II* structures. The overall picture suggests that there is a general mechanism of exchange that applies for this pair. A rigorous approach to the mechanism of coupling came from *ab initio* CASSCF/PT2 studies[39] and DFT studies[31] on a {Cu–Gd} dimer where the role of the 5d orbitals on the coupling mechanism was clearly established. Based on these studies, the following picture emerges: the net exchange interaction has two contributions – antiferromagnetic (J_{AF}) and ferromagnetic (J_F)

Table 1 Selected X-ray structural parameters of complexes **1–4**

Complexes	**1**	**2**	**3**	**4**
Ni_A–Gd	3.522	3.169	3.539	3.313
Ni_A–O	2.032 and 2.035	2.076, 2.077 and 2.106	2.042 and 1.979	2.062, 2.040 and 2.065
Gd– Ni_B	—	—	3.523	3.306
Ni_B–O	—	—	1.986 and 2.006	2.067, 2.086 and 2.048
Ni_A–O–Gd	106.5° and 107.9°	90°, 90.7° and 91.7°	107.6° and 107.3°	95.7°, 96.2° and 95.3°
Gd–O–Ni_B	—	—	106.9° and 108.2°	95°, 95.9° and 96°
Gd–O	2.318 and 2.354	2.368, 2.398 and 2.306	2.338, 2.404, 2.390 and 2.336	2.430, 2.379, 2.375, 2.405, 2.374, 2.392
Ni_A–O–Gd–O	2.8°	34.6°, 38.4° and 38.9°	15.3°	37.4°, 35.8° and 36.3°
Ni_B–O–Gd–O	—	—	16.7°	37.1°, 35.3° and 36.1°
Angle between Ni_A–O–Gd and Gd–O–Ni_B planes	—	—	57.6°	

Table 2 B3LYP computed J values on complexes **1–4**

Complexes	J_{calc} (cm^{-1})						J_{exp} (cm^{-1})		
	level I			*level II*					
1	+2.14			+1.84			+3.6		
2	+0.36			+0.71			+0.34		
1a[a]	–0.78			—			—		
1b[a]	–4.9			—			—		
Exchange	J_1	J_2	J_3	J_1	J_2	J_3	J_1	J_2	J_3
3	2.16	2.05	–0.15	0.89	0.74	–0.05	4.8	0.05	—
4[b]	0.59	0.56	–0.12	0.14	0.16	–0.01	0.91	0.91	—

[a] **1a** and **1b** are models of complex with ligand L^{1a} and L^{1b}. They represent modelled ligands where one/two of the bridging phenoxo oxygen atoms replaced by hydrogen atoms. Thus model **1a** and **1b** have one and no μ-OR bridging groups, respectively. [b] For complex **4**, there were two independent trinuclear units in the asymmetric unit, however the calculated J's are very similar for both structures ($J_1 = 0.59$, $J_2 = 0.56$ $J_3 = -0.12$ *vs.* the data presented in the table for other unit)

$$J = J_{AF} + J_F$$

For the {Ni–Gd} pair, the ferromagnetic contributions arise (i) from the interaction of the Ni^{II} magnetic orbitals with the empty Gd^{III} orbitals (5d and or 6 s) (ii) due to orbital orthogonality between 3d and 4f magnetic orbitals. The antiferromagnetic contributions solely arise due to the overlap between a pair of {3d–4f} magnetic orbitals. For the {Cu–Gd} pair, two such interactions have been detected from the CASSCF and DFT studies.[39,31] The 4f orbitals are not actively involved in the coupling mechanism compared to the 5d orbitals and this is similar to the fact that is established on the lanthanide catalysed reactions.[68]

The overlap integrals have been computed between the Ni^{II} magnetic orbitals (empty) and the Gd^{III} magnetic orbitals (empty) for complex **1** (choice of orbitals[43] and the computed overlap integrals are given in Table S3 and S4, ESI†). No significant overlap has been detected between the magnetic orbitals, revealing a near-complete orthogonality between the $d_{x^2-y^2}/d_{z^2}$ orbitals and the 4f orbitals of the Gd^{III} ions. Thus, the only source of antiferromagnetic contribution is negligible for **1**, leading to a strong ferromagnetic exchange. In order to probe the mechanism of coupling for the {Ni–Gd} pair, we have performed calculations on several model complexes of **1** and **2** and also computed the overlap integral between the pairs of magnetic orbitals and performed NBO analysis to establish and correlate the mechanism with the {Cu–Gd} pair. The exchange interactions computed for different model complexes (at *level I*) are listed in Table 2 (See also Fig. S1, ESI†). It is apparent from the calculations on model complexes presented in Table 2 that removing one or two μ-OR bridges leads to a net antiferromagnetic exchange. The change in J (ΔJ) on moving from the **1** to model **1a** is –2.85 cm^{-1} and to model 1b is –4.2 cm^{-1}. Thus the antiferromagnetic contribution to J increases tremendously upon a decrease in the number of bridging oxygen atoms. This is indirectly revealing an important clue regarding the mechanism of exchange that two or three μ-OR groups are essential to have ferromagnetic J values, as observed in the experimental results for a number of {Ni–Gd} complexes. When there is no bridge present (**1b**) between the two metals, unlike in the {Cu–Gd} pair where no interaction has been observed, a strong antiferromagnetic exchange has been computed. This is essentially due to the direct interaction of the dz^2 orbital of Ni^{II} with the f-orbitals of the Gd^{III} ions. To verify this statement, we have performed a correlation on **1b** where the Ni–Gd distance has been varied from 3.0 Å to 6.0 Å (see Fig. S2–S3, ESI†) and as expected, the antiferromagnetic interaction decreases with increasing the Ni–Gd distance and *vice versa*. The calculation of overlap integral reveals an increase in J_{AF} upon the removal of the μ-OR bridges. For model **1a**, three significant overlap integrals with the d_{z^2} orbital of Ni^{II} and 4f orbitals of Gd^{III} have been detected. For model **1b**, six such overlaps have been detected, with some of them having comparatively larger overlap integral values – especially the pairs having the d_{z^2} orbital of Ni^{II} ions. The NBO computed occupancy for complexes **1**, **1a** and **1b** are given in Table S5, ESI.† The partial occupancy of the 5d orbitals of Gd^{III} increases as we move from **1** to **1b**, but the occupation of the 4f orbitals and 6s orbitals of the Gd^{III} ions is nearly the same. This clearly reveals a correlation of J with the 5d occupation while the 6s is orbital is likely to be a silent spectator on the exchange mechanism.[31]

For complex **2**, two significant overlaps (with d_{z^2} and $d_{x^2-y^2}$ orbitals; See Fig. 2) have been detected revealing a non-orthogonality between the {3d–4f} orbitals, unlike in **1**. The ferromagnetic contribution J_F also decreases compared to that of **1**, as revealed by the NBO analysis. This leads to a significant reduction in the net exchange interaction. For complex **2** similar models have also been constructed (**2a–c**, see ESI†) and the overlap integral calculations reveal many significant overlaps leading to an increase in J_{AF} and hence a net antiferromagnetic interaction.

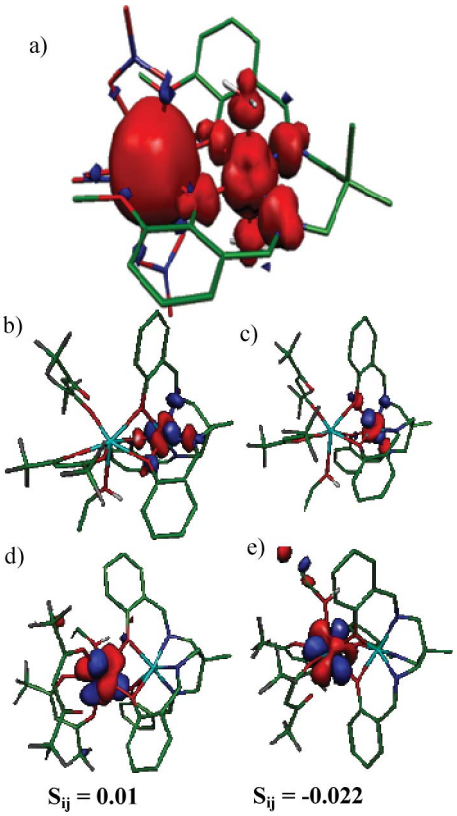

Fig. 2 a) DFT computed spin density plot of **1** for $S = 9/2$ state. The isodensity surface represented corresponds to a value of 0.0012 e^-/bohr3. The red and blue region indicates positive and negative densities, respectively. b) $d_{x^2-y^2}$ and c) d_{z^2} magnetic orbitals of Ni^{II} atoms in complex **1**. d–e) representative magnetic orbitals of Gd^{III} with their corresponding overlap integral values with d) $d_{x^2-y^2}$ e) d_{z^2} orbitals of Ni^{II} ions.

The computed exchange interactions in all model complexes are predicted to be antiferromagnetic in nature. This reveals a subtle interplay in the mechanism of coupling in these complexes. A similar study on the model complexes has been performed by one of us previously on the {Cu–Gd} dinuclear complex, where an antiferromagnetic exchange for a single μ-OR bridge complex has been predicted.[31] Although no single μ-OR bridged 3d–4f complexes have been reported so far, a single μ-oximato bridged {Cu–Gd} dimer recently reported has antiferromagnetic coupling and this supports our predictions.[69]

The computed spin density plot together with the magnetic orbitals of Ni^{II} of complex **1** is shown in Fig. 2. The spin density on the Ni^{II} (1.663) is delocalised to other atoms while in the Gd^{III} (7.028) ion, the unpaired electrons are fully localised. A slight increase from the expected value in the spin density is due to the spin polarization mechanism. The two nitrogen atoms coordinated to the Ni^{II} and the two bridging oxygen atoms have positive spin densities (0.089 and 0.084 on the nitrogens and 0.051 and 0.049 on the oxygens) due to predominant delocalization mechanisms.[33–38] The oxygen atoms coordinated to the Gd^{III} ions have small negative spin density due to the predominant spin polarization mechanism (from –0.001 to –0.003). Smaller spin density values found on the bridging oxygens (~0.05) compared to that of the nitrogen atoms (~0.08) is due to a competing spin delocalisation from the Ni^{II} and spin polarisation from the Gd^{III} atoms (see Fig. S5–S6 and Tables S6–S7 for the computed spin densities on selected atoms, ESI†).

3.3 Magneto-structural correlations in dinuclear {Ni–Gd} complexes

The magneto-structural correlations are important means of interpreting the observed magnetic properties of novel and/or more complex compounds in order to design new compounds with expected magnetic properties. Three magneto-structural correlations have been performed on complex **1** by varying bond angles, bond lengths and dihedral angles.

Bond angle. The first correlation is developed by varying Ni–O–Gd bond angles. The average Ni–O–Gd bond angle *vs.* J plot is shown in Fig. 3a. The angle and the J values are correlated by an exponential function, $J = Ae\left(\frac{-x}{t}\right) + y_0$ where $y_0 = 5.50118$, $A = -28.62337$, $t = 50.98665$ and x is the Ni–O–Gd bond angle. As the bond angle increases, the J value becomes more ferromagnetic. At lower angles, the structure is more compact and the overlap between magnetic orbitals increases. The calculation of overlap integrals between the 3d and the 4f orbitals reveals a significant overlap for lower bond angle structures disclosing an increase in the antiferromagnetic contribution to the net exchange interaction. Additionally, a decrease in bond angle leads to an inefficient charge transfer from the 3d orbital of the Ni^{II} to the 5d orbitals of the Gd^{III} ions. Thus a decrease in the J_F contribution is also expected. The spin density values of the Ni^{II} ions are plotted against the average Ni–O–Gd angle and are shown in Fig. 3b. The spin densities on the Ni^{II} centres increases with the increase in the angle up to 110°. Afterwards, the spin density decreases slightly. The increase in spin density means less delocalization and this correlates with the increase in ferromagnetic coupling observed in Fig. 3a. The experimental J values together with their corresponding average Ni–O–Gd angles are plotted together with the computed data in Fig. 3a (red circles).

Although some deviations were found, a general trend has been observed where larger angles lead to larger exchange interaction. Interestingly, this correlation predicts an antiferromagnetic {Ni–Gd} interaction for bond angle less than 84° and this strikingly correlates with the antiferromagnetic {Ni–Gd} exchange reported for a structure with bond angle of 85.7° having the J value of –0.22 cm^{-1}.

Bond distance. The second correlation is developed by varying the Ni–O and the Gd–O distances. The plot of average Ni–O and Gd–O distance against J is shown in Fig. 3c. In this case, a linear relationship has been found (see inset of Fig. 3c for constants of the equations). As the bond distance increases, the ferromagnetic interaction decreases. This behaviour is somewhat

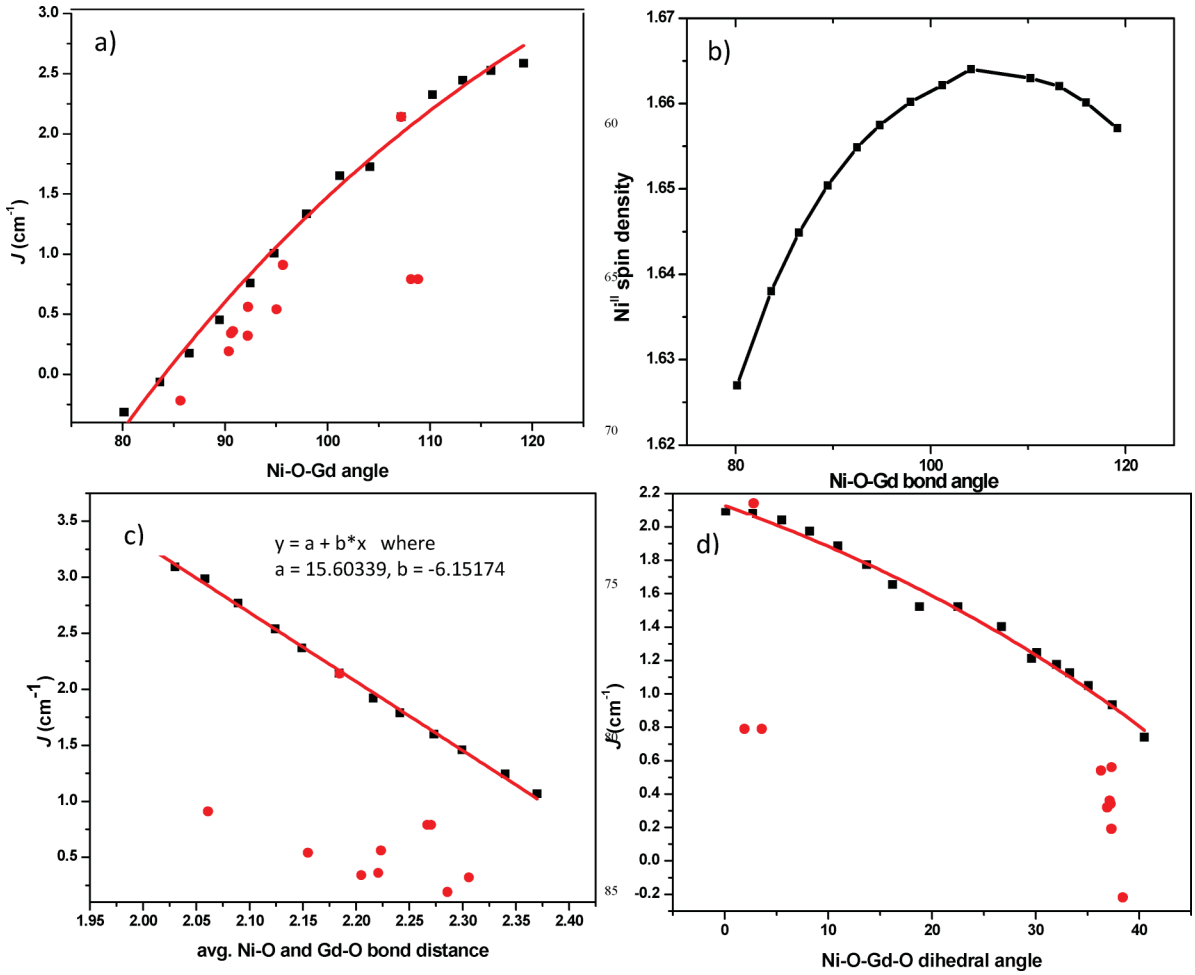

Fig. 3 Magneto-structural correlation developed by DFT calculations by varying different structural parameters. a) Ni–O–Gd bond angle. b) Computed spin-densities plotted against the Ni–O–Gd bond angle c) average Ni–O and Gd–O bond distances d) Ni–O–Gd–O dihedral angle on complex **1**.

expected; as the Ni–O and or Gd–O bond elongates, it effectively reduces the charge transfer path of Ni(3d)→Gd(5d) orbitals and thus the ferromagnetic contribution to the total J decreases. The comparison with the experimental data reveals that bond distances are not unique parameters in determining the magnitude (and also the sign) of the exchange constant.

Dihedral angle. Consequently the third correlation is developed by varying the Ni–O–Gd–O torsional angle (Fig. 3d).

This correlation again shows an exponential dependence similar to bond angle correlation (here $y_0 = 3.33544$, $A = -1.20769$ and $t = -54.0927$). From Fig. 3d, it is clear that the planar structure having zero torsional angle has the largest ferromagnetic exchange. Larger torsional angle leads to a lower J value, similar to that found for the {Cu–Gd} pair. The experimental points are rather scattered here and presumably suggest that the dihedral angle might not be the only structural parameter which controls the magnetic exchange.

For complex **2**, the bond distance and angle are expected to behave in a similar fashion to complex **1**, but the dihedral correlation is expected to be different as there are three μ-OR bridges. In complex **2**, as there are three different torsional angles, we have developed a correlation on this complex by varying two dihedral angles at a time and this correlation is given in Fig. S4, ESI.† This correlation also indicates that the antiferromagnetic contribution increases upon an increase in the dihedral angle.

In general, *type I* structures have larger J values than *type II* structures.[40,51] From the computation and the developed magneto-structural correlations, it is apparent that the reason for smaller J values in the *type II* structures are due to the acute Ni–O–Gd angles observed in these structures. The acute angle results due to the presence of three μ-OR bridges. Although other structural parameters such as Ni–O–Gd–O dihedral angles also differ between the two structural motifs, for the {Ni–Gd} pair the bond angle seems to be a more reliable parameter to correlate with the J values.

3.4 Exchange interactions in trinuclear {Ni–Gd–Ni} complexes

Since {Ni–Gd} topology ensures ferromagnetic interactions between the metal ions, the nuclearity has been extended by incorporating another Ni ion into the cluster aggregation to produce {Ni–Gd–Ni} trinuclear complexes where the ground state S value increases from 9/2 to 11/2. This strategy has been adapted to the synthesis of many novel trinuclear and higher nuclearity clusters to produce large S values.[47,48,50] In trinuclear complexes, apart from two near-neighbour {Ni–Gd}

interactions, the {Ni–Ni} interaction also plays a prominent role in stabilising the spin ground state.[48,50] This next-nearest-neighbour 1,3 interactions, although present in 3d transition metal clusters, are usually ignored as they are weak compared to the near-neighbour interactions. However, in {3d–4f} complexes, these interactions are important because (i) the near-neighbour interactions are relatively weak and (ii) the 4f ions have larger diffused empty orbitals and these orbitals could play an important role in mediating a coupling between the two metal (here Ni^{II}) centres. In order to shed light on the nature and characteristics of these two interactions, we have extended our studies to trinuclear {Ni–Gd–Ni} complexes having structural motifs *type Ia* and *type IIb*, as shown in Scheme 1. Here we have performed DFT calculations on the full structures of $[(L^3Ni(H_2O))_2Gd(H_2O)](CF_3SO_3)_3$ (**3**) (L^3=N,N'-2,2-dimethylproppylenedi(3-methoxosalicylidene iminiato) and $[(L^4Ni)_2Gd](NO_3)$ (**4**) (L^4 = triamine 1,1,1-tris(aminomethyl)ethane) to probe the difference in structural motifs that would lead to a difference in the coupling strength. The important structural parameters that would affect the exchange interactions are listed in Table 1. The structural parameters of complex **3** are similar to that of **1** except that the Ni–O–Gd–O dihedral angle is larger for complex **3** compared to complex **1**. The Ni–O–Gd angles are very similar and so is the computed {Ni–Gd} interaction between complexes **1** and **3**.

The computed J_1–J_3 (see inset of Fig. 1 for description) for complexes **3** and **4** are listed in Table 2. The computation reveals that both the {Ni–Gd} interactions (J_1 and J_2) are ferromagnetic in nature while the 1,3 {Ni–Ni} interaction is antiferromagnetic in nature. The magnitude of the {Ni–Gd} interaction is smaller for complex **4** compared to **3**, as expected due to the differences in the structural motifs (*type Ia vs. type IIb*). The experimental exchange coupling for complex **3** is found to be J_1 = 4.8 cm^{-1} and J_2 = 0.05 cm^{-1}.[40] For complex **3**, the authors claim that the $J_1 = J_2$ does not yield a good fit to the magnetic susceptibility data, while allowing J_1 and J_2 to be different provided a good fit. This difference in the strength of J led them to conclude that the empty 5d orbitals might participate in the exchange mechanism. Since the experimental and theoretical values contradict each other as calculations revealing $J_1 \approx J_2$ scenario, we have probed the possible source of error in this case by seeking additional information from the X-ray structure, simulations and additional computations. The {Ni–Gd} interaction in complex **3** is related to one of the structural parameters we discussed earlier (bond lengths, bond angles and dihedral angles). It is apparent from Table 1 that the structural parameters for the {Ni_A–Gd} (J_1) and {Gd–Ni_B} (J_2) are very similar. Substituting these structural parameters to the correlations developed earlier for the dimer provides $J_1 \approx J_2 \approx 2$ cm^{-1}. Our theoretical calculations at *level I* and *level II* consistently reveal that $J_1 \approx J_2$ (see Table 2). We have also performed additional DFT calculations on model complexes by replacing one of the Ni^{II} ions by Zn^{II} (Ni_A–Gd–Zn and Zn–Gd–Ni_B to calculate J_1 and J_2 independently). Here we obtain $J_1 = 2.14$ and $J_2 = 2.06$, again revealing a similar $J_1 \approx J_2$ strength. In addition to J_1 and J_2 interactions, we also have a very weak J_3 interaction which is antiferromagnetic in nature. At lower temperatures this can be significant, therefore we have performed simulation of the magnetic data using the DFT computed J values (*level I*). In addition to the exchange coupling constants, single-ion zero-field splitting for the Ni_A and Ni_B atoms have been taken into account and this yields an excellent fit (See Figure S7, ESI†) and this also indicates that $J_1 \approx J_2$ and inclusion of the J_3 {Ni–Ni} interaction is important and this can not be ignored completely as it is antiferromagnetic in nature.

For complex **4**, the DFT computed J values are in good accord to the experimental J's. As expected the strength of the interaction diminishes compared to that of complex **3** due to smaller Ni–O–Gd angles present in this structure. A weak antiferromagnetic J_3 was also observed for complex **4**.

The mechanism of magnetic coupling proposed for the dinuclear {Ni–Gd} complexes also holds for the trinuclear complexes. A structurally similar Ni^{II} ion on both sides of Gd^{III} ions and the participation of empty 5d orbitals of the Gd^{III} in the mechanism basically ensures that the interaction on both sides ({Ni_A–Gd} and (Gd–Ni_B}) should have same sign of exchange coupling (See Scheme 2). The partial charge transfer from Ni_A to Gd empty 5d orbitals ensures that the structurally similar other half should have the same spin as that of the partially occupied 5d orbitals, leading to coupling of the same sign for both the {Ni_A–Gd}and {Gd–Ni_B} pairs.

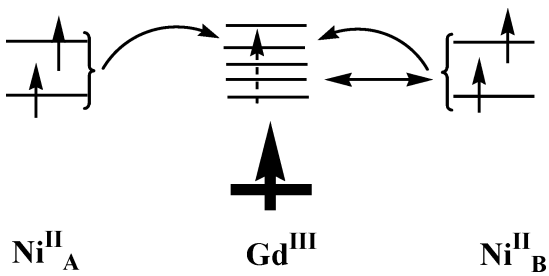

Scheme 2 A schematic exchange mechanism for the {Ni–Gd–Ni} complexes.

The computed spin density distribution for the high spin state of complex **3** is shown in Fig. 4. The spin density on the Gd^{III} ion is found to be 7.025 while on the Ni_A and Ni_B are 1.652 and 1.656 respectively. A small difference in the Ni^{II} spin densities is associated with the very small difference in the coupling strength computed. The delocalisation and polarisation mechanisms are found to be operative around the coordination sphere of Gd^{III} and this is similar to that discussed earlier for the dinuclear complex.

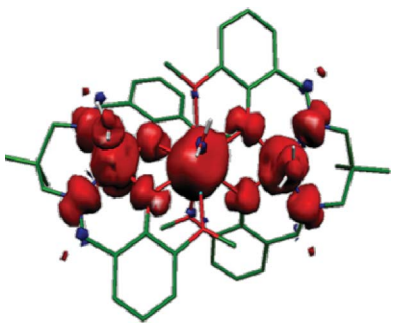

Fig. 4 Representation of spin densities corresponding to the ferromagnetic S = 11/2 ground state of complex **3**. The isodensity surface represented corresponds to a value of 0.0012 e^- / $bohr^3$. The red and blue regions indicate positive and negative spin populations, respectively.

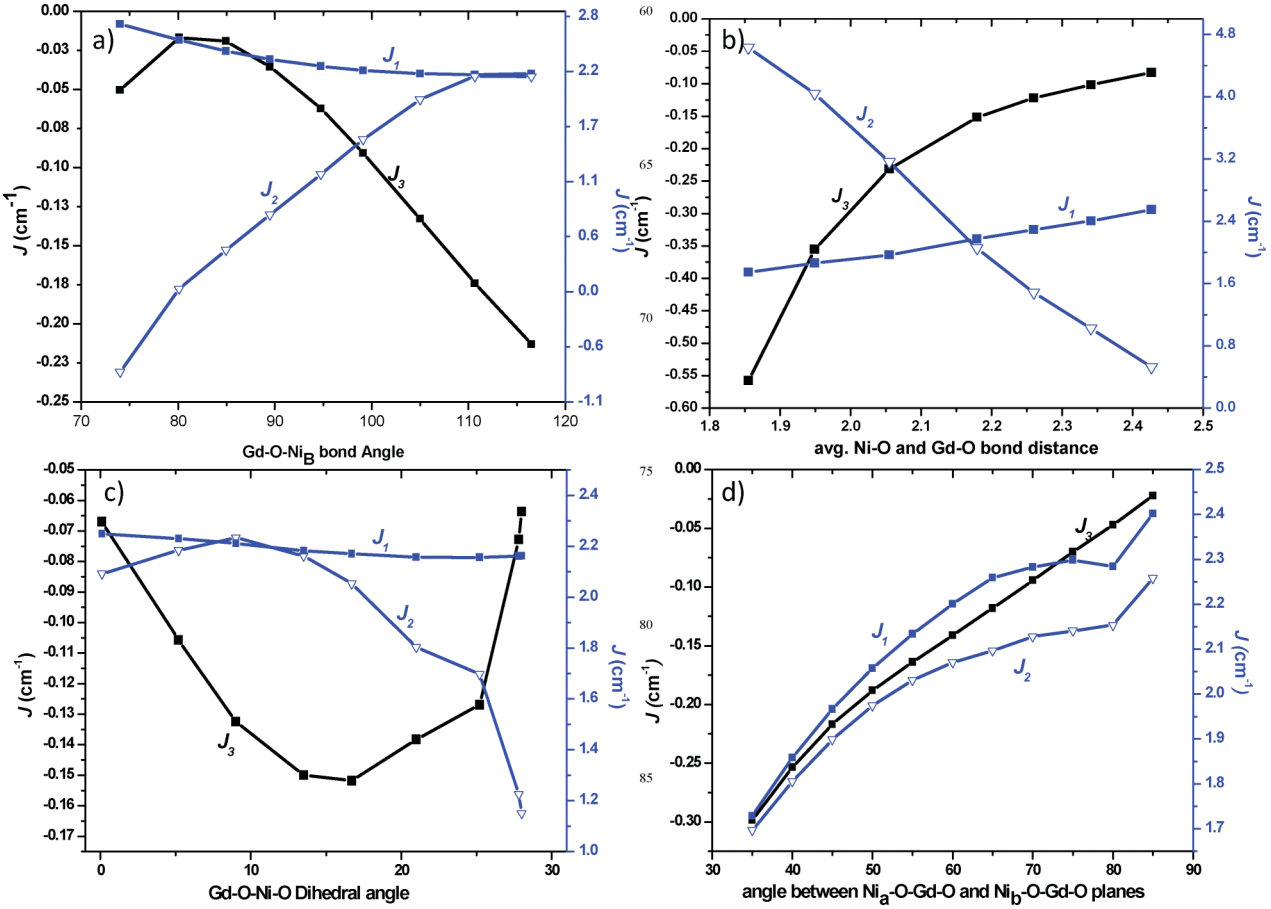

Fig. 5 Magneto-structural correlations developed by varying different structural parameters a) Ni_B–O–Gd bond angle. b) average Ni–O and Gd–O distance c) Ni_B–O–Gd–O dihedral angle. d) angle between Ni_A–O_2–Gd and Gd–O–Ni_B planes.

3.5 Magneto-structural correlations in trinuclear {Ni–Gd–Ni} complexes

We have also developed magneto-structural correlations[70] for trinuclear {Ni–Gd–Ni} complex **3**, essentially to understand the behaviour of the {Ni–Gd} interactions and more importantly the behaviour of the {Ni–Ni} interactions. We have developed correlations for bond lengths, bond angles and dihedral angles (see Fig. 5). In order to track the changes and to be able to compare it with the dinuclear complexes, we have modified only the structural parameters around the {$GdNi_B$} unit while the {Ni_AGd} structural parameters were kept constant. Since the mechanism of exchange coupling here is governed by many factors, these type of correlations are useful to understand the co-operativity if any, between the pairs.

Bond angle. The correlation developed by varying the Gd–O–Ni_B angle from 74° to 119° is shown in Fig. 5a. It is clear from this figure that the J_1 interaction is nearly constant as the structural parameters around the {Ni_AGd} are unaltered. Similar to the dinuclear correlation, an increase in bond angle increases the ferromagnetic J_2. Even antiferromagnetic J_2 has been detected at very small angles. The behaviour of the J_3 interaction is different as it increases initially and then reaches a maximum and then tends to decrease at larger angles. The sign of J_3 is retained at all computed points and at larger angles it becomes moderately antiferromagnetic.

Bond distance. Second magneto-structural correlation was performed by varying the average Ni_B–O and Gd–O (Fig. 5b) distances. The J_1 interaction is nearly constant while J_2 decreases with an increase in the bond length. The J_3 however reaches close to zero at very large distances and at short distances, the interaction is strongly antiferromagnetic. In order to understand this interaction further another graph has been plotted (see Fig. S8b, ESI†) where the Ni_A–Ni_B distance against J_3 is plotted (Note here that varying the Ni_B–O and Gd–O distances lead to an increase in Ni_A–Ni_B distance). Here it is clearly apparent that the J_3 interaction decreases with an increase in Ni_A–Ni_B distance as one would expect.

Dihedral angle. A third correlation was performed by changing the Ni_B–O–Gd dihedral angle from 0° to 29°. As we move from lower dihedral angle to larger values, the J_2 increases slightly to 10° but afterwards it decreases (see Fig. 5c). In this correlation the J_3 initially decreases with an increase in dihedral angle up to 15°. However, beyond 15° the J_3 increases. Here J_3 shows a parabolic shape.

Twist angle. For trinuclear complexes, an additional correlation exists where the two dihedral planes (Ni_A–O–Gd–O and

Gd–O–Ni_B–O) can be twisted without affecting other structural parameters (see Scheme 3). The developed correlation is shown in Fig. 5d. In the X-ray structure, the two planes are already twisted with a twist angle of 57.6°. All three exchange interactions show a similar trend where the magnitude of the J increases with an increase in the twist angle (see Fig. S8a for a spin density dependent plot across the twist angle, ESI†). It is important to note that this and other correlations developed reveals that J_1–J_3 are correlated with each other as demonstrated in this magneto-structural correlation. This is similar to metal–radical coupling observed for other systems.[71]

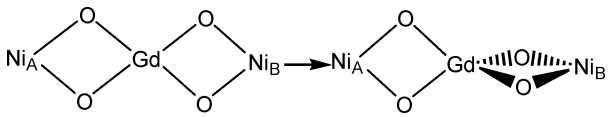

Scheme 3

4. Conclusions

In recent years there has been a great deal of interest in the synthesis and magnetic studies of mixed {3d–4f} complexes. Despite numerous experimental reports, very little work has been done on the theoretical side to understand or to predict the magnetic properties of this type of complex. Here we have studied for the first time two dinuclear {Ni–Gd} and two trinuclear {Ni–Gd–Ni} complexes with two and three μ–OR groups. The conclusions derived from this work can be summarised as follows:

(i) studies on complexes **1–4** possessing different structural topology and different exchange constants reveals that the combination of B3LYP with an effective core potential basis set on Gd^{III} provides an accurate description of ferromagnetic coupling present in these complexes and yields an excellent estimate of the magnetic exchange constants compared to experiments.

(ii) MO, NBO and studies on model complexes reveal that the empty 5d orbitals of Gd^{III} play an important role in the mechanism of coupling. Unlike the {Cu–Gd} pair,[31,40] a large antiferromagnetic interaction has been observed for the naked model, indicating the possibility of reaching a large antiferromagnetic interaction in this type of complex.

(iii) two types of {Ni–Gd} structural cores have been studied, one with two μ-OR groups and the other with three. Large differences in the J between these two structural motifs are attributed to the difference in the Ni–O–Gd angles.

(iv) although only a limited set of experimental data are available to check the most reliable parameter on which the J is strongly correlated, there is a clear indication that the Ni–O–Gd angles play a prominent role here and this parameter governs the ferro-antiferromagnetic switch in this type of complex. An exponential relation for bond angle *vs.* J has been computed with a larger angles favouring ferromagnetic interaction.

(v) for trinuclear complexes, the {Ni–Ni} 1,3 interaction is found to be small but it is antiferromagnetic in nature. The large discrepancy between the computed and experimental J for complex **3** could be due to the negligible J_3 {Ni–Ni} interaction in the experimental fitting.

(vi) extensive magneto-structural correlations have been developed for trinuclear complexes to understand the behaviour of the {Ni–Ni} interactions as this interaction seems to prevail over the ferromagnetic {Ni–Gd} interactions in polynuclear complexes. Our studies reveal that, although this interaction is small in magnitude, it is antagonistic to the behaviour of the {Ni–Gd} interaction in the list of parameters studied here.

(vii) magneto-structural correlations which are specific to trinuclear complexes have also been developed and the dihedral twist parameter between the two dimeric {Ni–Gd} units seems to be an important parameter.

Although the mechanism of coupling in the {Ni–Gd} dimer has been established and magneto-structural correlations have been developed in this work, the mechanism and correlations for other {3d–4f} dimers are expected to be different and we are currently working on this issue.

Acknowledgements

Financial support from the Government of India through the Department of Science and Technology (SR/S1/IC-41/2010), Indian Institute of Technology, Bombay, for the seed grant and access to the high performance computing facility are gratefully acknowledged.

Notes and references

1 R. Sessoli, D. Gatteschi, A. Caneschi and M. A. Novak, *Nature*, 1993, **365**, 141; G. Christou, D. Gatteschi, D. N. Hendrickson and R. Sessoli, *Mater. Res. Bull.*, 2000, **25**, 66; D. Gatteschi, R. Sessoli and J. Villain, *'Molecular Nanomagnets'*, Oxford University Press, Oxford, 2006.
2 M. Leuenberger and D. Loss, *Nature*, 2001, **410**, 6830; S. Hill, R. S. Edwards, N. Alliaga-Alcalde and G. Christou, *Science*, 2003, **302**, 1015; M. Affronte, F. Troiani, A. Ghirri, A. Candini, M. Evangelisti, V. Corradini, S. Carretta, P. Santini, G. Amoretti, F. Tuna, G. Timco and R. E. P Winpenny, *J. Phys. D: Appl. Phys.*, 2007, **40**, 2999; R. E. P. Winpenny, *Angew. Chem., Int. Ed.*, 2008, **6**, 7992.
3 F. K. Larsen, E. J. L. McInnes, H. El. Mkami, J. Overgaard, S. Piligkos, G. Rajaraman, E. Rentschler, A. A. Smith, G. M. Smith, V. Boote, M. Jennings, G. A Timco and R. E. P. Winpenny, *Angew. Chem., Int. Ed.*, 2003, **42**, 101; M. Affronte, F. Troiani, A. Ghirri, S. Carretta, P. Santini, V. Corradini, R. Schuecker, C. Muryn, G. Timco and R. E. P. Winpenny, *Dalton Trans.*, 2006, 2810; F. Troiani, A. Ghirri, M. Affronte, S. Carretta, P. Santini, G. Amoretti, S. Piligkos, G. Timco and R. E. P. Winpenny, *Phys. Rev. Lett.*, 2005, **94**, 207208.
4 C. J. Milios, R. Inglis, A. Vinslava, R. Bagai, W. Wernsdorfer, S. Parsons, S. P. Perlepes, G. Christou and E. K. Brechin, *J. Am. Chem. Soc.*, 2007, **129**, 12505; C. J. Milios, A. Vinslava, W. Wernsdorfer, A. Prescimone, P. A. Wood, S. Parsons, S. P. Perlepes, G. Christou and E. K. Brechin, *J. Am. Chem. Soc.*, 2007, **129**, 6547; C. J. Milios, A. Vinslava, W. Wernsdorfer, S. Moggach, S. Parsons, S. P. Perlepes, G. Christou and E. K. Brechin, *J. Am. Chem. Soc.*, 2007, **129**, 2754.
5 R. Sessoli and A. Powell, *Coord. Chem. Rev.*, 2009, **253**, 232.
6 S.-D. Jiang, B.-W. Wang, G. Su, Z.-M. Wang and S. Gao, *Angew. Chem., Int. Ed.*, 2010, **49**, 7448.
7 M. A. AlDamen, J. M. Clemente-Juan, E. Coronado, C. Mari-Gastaldo and A. Gaito-Arina, *J. Am. Chem. Soc.*, 2008, **130**, 8874.
8 N. Ishikawa, M. Sugita, T. Ishikawa, S.-Y. Koshihara and Y. Kaizu, *J. Phys. Chem. B*, 2004, **108**, 11265.
9 N. Zhou, Y. Ma, C. Wang, G. Xu. Feng, J.-K. Tang, J.-X. Xu, S.-P. Yan and D.-Z. Liao, *Dalton Trans.*, 2009, 8489.
10 Po-Heng Lin, T. J. Burchell, L. Ungur, L. F. Chibotaru, W. Wernsdorfer and M. Murugesu, *Angew. Chem., Int. Ed.*, 2009, **48**, 9489.
11 C. Zaleski, E. Depperman, J. Kampf, M. Kirk and V. Pecoraro, *Angew. Chem., Int. Ed.*, 2004, **43**, 3912.
12 A. Mishra, W. Wernsdorfer, S. Parsons, G. Christou and E. K. Brechin, *Chem. Commun.*, 2005, 2086.
13 M. Murugesu, A. Mishra, W. Wernsdorfer, K. A. Abboud and G. Christou, *Polyhedron*, 2006, **25**, 613.

14 V. M. Mereacre, A. M. Ako, R. Clérac, W. Wernsdorfer, G. Filoti, J. Bartolomé, C. E. Anson and A. K. Powell, *J. Am. Chem. Soc.*, 2007, **129**, 9248.
15 J. Rinck, G. Novitchi, W. Van Den Heuvel, L. Ungur, Y. Lan, W. Wernsdorfer, C. E. Anson, L. F. Chibotaru and A. K. Powell, *Angew. Chem., Int. Ed.*, 2010, **49**, 7583.
16 J.-P. Costes, F. Dahan, B. Donnadieu, M. I. Feranadez-Garcia and M. J. Rodriguez-Douton, *Dalton Trans.*, 2003, 3776.
17 J.-P. Costes, F. Dahan and J. Garcia-Tojal, *Chem.–Eur. J.*, 2002, **8**, 5430.
18 J.-P. Costes, F. Dahan, A. Dupuis and J. P. Laurent, *Inorg. Chem.*, 1997, **36**, 4284.
19 T. Yamaguchi, Y. Sunatsuki, M. Kojima, H. Akashi, M. Tsuchimoto, N. Re, S. Osa and N. Matsumoto, *Chem. Commun.*, 2004, 1048.
20 J.-P Costes, F. Dahan, F. Dumestre, J. M. Clemente-Juan and J. P. Tuchagues, *Dalton Trans.*, 2003, 464.
21 J. P. Costes, A. Dupuis and J. P. Laurent, *J. Chem. Soc., Dalton Trans.*, 1998, 735.
22 M. Evangelisti and E. K. Brechin, *Dalton Trans.*, 2010, 4672; S. K. Langley, N. F. Chilton, B. Moubaraki,T. Hooper,E. K. Brechin,M. Evangelisti and K. S. Murray, *Chem. Sci.*, 2011, DOI: 10.1039/c1sc00038a.
23 E. Ruiz, S. Alvarez, A. Rodriguez-Fortea, P. Alemany, Y. Pouillon and C. Massobrio, in *"Magnetism: Molecules to Materials"*, Vol. II ed J. S. Miller and M. Drillon, Wiley-VCH, Weinheim, 2001, pp 227.
24 A. Bencini and F. Totti, *Int. J. Quantum Chem.*, 2005, **6**, 819.
25 G. Rajaraman, M. Murugesu, E. C. Sanudo, M. Soler, W. Wernsdorfer, M. Helliwell, C. Muryn, J. Raftery, S. J. Teat, G. Christou and E. K. Brechin, *J. Am. Chem. Soc.*, 2004, **126**, 15445.
26 S. Piligkos, G. Rajaraman, M. Soler, N. Kirchner, J. van Slageren, R. Bircher, S. Parsons, H. Guedel, J. Kortus, W. Wernsdorfer, G. Christou and E. K. Brechin, *J. Am. Chem. Soc.*, 2005, **127**, 5572.
27 K. Hegetschweiler, B. Morgenstern, J. Zubieta, P. J. Hagrman, N. Lima, R. Sessolia and F. Totti, *Angew. Chem., Int. Ed.*, 2004, **43**, 3436.
28 I. Rudra, C. Raghu and S. Ramasesha, *Phys. Rev. B: Condens. Matter*, 2002, **65**, 224411.
29 E. Ruiz, T. Cauchy, J. Cano, R. Costa, J. Tercero and S. Alvarez, *J. Am. Chem. Soc.*, 2008, **130**, 7420; E. Ruiz, J. Cirera, J. Cano, S. Alvarez, C. Loose and J. Kortus, *Chem. Commun.*, 2008, 52; E. Ruiz, *Structure and Bonding*, Springer, Berlin, Germany, 2004, 113.
30 J. Kortus, M. R. Pederson, T. Baruah, N. Bernstein and C. S. Hellberg, *Polyhedron*, 2003, **22**, 1871.
31 G. Rajaraman, F. Totti, A. Bencini, A. Caneschi, R. Sessoli and D. Gatteschi, *Dalton Trans.*, 2009, 3153.
32 C. Benelli, A. Caneschi, D. Gatteschi, O. Guillou and L. Pardi, *Inorg. Chem.*, 1990, **29**, 1750.
33 A. Bencini, C. Benelli, A. Caneschi, A. Dei and D. Gatteschi, *Inorg. Chem.*, 1985, **25**, 572.
34 D. Gatteschi, *Adv. Mater.*, 1994, **6**, 635; C. Benelli, A. Caneschi, D. Gatteschi and R. Sessoli, *J. Appl. Phys.*, 1993, **73**, 5333.
35 C. Benelli, A. Caneschi, A. Fabretti, D. Gatteschi and L. Pardi, *Inorg. Chem.*, 1990, **29**, 4153.
36 O. Kahn and O. Guillou, in *Reserach Frontiers in Magnetochemistry*, ed. C. J. O'Conner, World Scientific, Singapore, 1993, pp 179; O. Kahn, *Angew. Chem., Int. Ed. Engl.*, 1985, **24**, 834.
37 I. Ramada, O. Kahn, Y. Jeannin and F. Robert, *Inorg. Chem.*, 1997, **36**, 930; O. Guillou, P. Bergerat, O. Kahn, E. Bakalbassis, K. Boubekeur, P. Batail and M. Guillot, *Inorg. Chem.*, 1992, **31**, 110.
38 O. Kahn, *Molecular Magnetism*, VCH Publishers, New York, 1993.
39 V. Paulovic, F. Cimpoesu, M. Ferbinteanu and K. Hirao, *J. Am. Chem. Soc.*, 2004, **126**, 3321.
40 J-P. Costes, T. Yamaguchi, M. Kojima and L. Vendier, *Inorg. Chem.*, 2009, **48**, 5555.
41 J. Cirera and E. Ruiz, *C. R. Chimie.*, 2008, **11**, 1227.
42 C. Desplanches, E. Ruiz, A. Rodríguez-Fortea and S. Alvarez, *J. Am. Chem. Soc.*, 2002, **124**, 5197.
43 Please note here that as reported earlier,[41,42] the empty "magnetic orbitals" of the broken-symmetry solution are the best choice to compute the overlap-integral as the occupied magnetic orbitals are difficult to determine due to strong mixing with the ligand orbitals.
44 J.-P. Costes and L. Vendier, *Eur. J. Inorg. Chem.*, 2010, **18**, 2768.
45 J.-P. Sutter, S. Dhers, R. Rajamani, S. Ramasesha, J.-P. Costes, C. Duhayon and L. Vendier, *Inorg. Chem.*, 2009, **48**, 5820.
46 J. Titis and R. Boca, *Inorg. Chem.*, 2010, **49**, 3971.
47 S. Igarashi, S. Kawaguchi, Y. Yukawa, F. Tuna and R. E. P. Winpenny, *Dalton Trans.*, 2009, 3140.
48 C. G. Efthymiou, T. C. Stamatatos, C. Papatriantafyllopoulou, A. J. Tasiopoulos, W. Wernsdorfer, S. P. Perlepes and G. Christou, *Inorg. Chem.*, 2010, **49**, 9737.
49 C. A. Barta, S. R. Bayly, P. W. Read, B. O. Patrick, R. C. Thompson and C. Orvig, *Inorg. Chem.*, 2008, **47**, 2280.
50 Y. Yukawa, G. Aromi, S. Igarashi, J. Ribas, S. A. Zvyagin and J. Krzystek, *Angew. Chem., Int. Ed.*, 2005, **44**, 1997.
51 A. N. Georgopoulou, R. Adam, C. P. Raptopoulou, V. Psycharis, R. Ballesteros, B. Abarca and A. K. Boudalis, *Dalton Trans.*, 2010, 5020.
52 L. Noodleman, *J. Chem. Phys.*, 1981, **74**, 5737.
53 E. Ruiz, S. Alvarez, J. Cano and P. Alemany, *J. Comput. Chem.*, 1999, **20**, 1391; E. Ruiz, A. R. Fortea, J. Cano, S. Alvarez and P. Alemany, *J. Comput. Chem.*, 2003, **24**, 982; E. Ruiz, J. Cano, S. Alvarez, A. Caneschi and D. Gatteschi, *J. Am. Chem. Soc.*, 2003, **152**, 6791; G. Rajaraman, J. Cano, E. K. Brechin and E. J. L. McInnes, *Chem. Commun.*, 2004, 1476.
54 P. Christian, G. Rajaraman, A. Harrison, M. Helliwell, J. J. W. McDouall, J. Raftery and R. E. P. Winpenny, *Dalton Trans.*, 2004, 2550.
55 *Gaussian 03, Revision C.01*, M. J. Frisch, G. W. Trucks, H. B. Schlegel, G. E. Scuseria, M. A. Robb, J. R. Cheeseman, J. A. Montgomery, Jr., T. Vreven, K. N. Kudin, J. C. Burant, J. M. Millam, S. S. Iyengar, J. Tomasi, V. Barone, B. Mennucci, M. Cossi, G. Scalmani, N. Rega, G. A. Petersson, H. Nakatsuji, M. Hada, M. Ehara, K. Toyota, R. Fukuda, J. Hasegawa, M. Ishida, T. Nakajima, Y. Honda, O. Kitao, H. Nakai, M. Klene, X. Li, J. E. Knox, H. P. Hratchian, J. B. Cross, V. Bakken, C. Adamo, J. Jaramillo, R. Gomperts, R. E. Stratmann, O. Yazyev, A. J. Austin, R. Cammi, C. Pomelli, J. W. Ochterski, P. Y. Ayala, K. Morokuma, G. A. Voth, P. Salvador, J. J. Dannenberg, V. G. Zakrzewski, S. Dapprich, A. D. Daniels, M. C. Strain,O. Farkas,D. K. Malick, A. D. Rabuck, K. Raghavachari, J. B. Foresman, J. V. Ortiz, Q. Cui, A. G. Baboul, S. Clifford, J. Cioslowski, B. B. Stefanov, G. Liu, A. Liashenko, P. Piskorz, I. Komaromi, R. L. Martin, D. J. Fox, T. Keith, M. A. Al-Laham, C. Y. Peng, A. Nanayakkara, M. Challacombe, P. M. W. Gill, B. Johnson, W. Chen, M. W. Wong, C. Gonzalez and J. A. Pople, 2004, Gaussian, Inc., Wallingford CT.
56 A. D. Becke, *J. Chem. Phys.*, 1993, **98**, 5648.
57 T. R. Cundari and W. J. Stevens, *J. Chem. Phys.*, 1993, **98**, 5555.
58 P. J. Hay and W. R. Wadt, *J. Chem. Phys.*, 1985, **82**, 270; P. J. Hay and W. R. Wadt, *J. Chem. Phys.*, 1985, **82**, 284; P. J. Hay and W. R. Wadt, *J. Chem. Phys.*, 1985, **82**, 299.
59 R. Ditchfield, W. J. Hehre and J. A. Pople, *J. Chem. Phys.*, 1971, **54**, 724; V. A. Rassolov, M. A. Ratner, J. A. Pople, P. C. Redfern and L. A. Curtiss, *J. Comput. Chem.*, 2001, **22**, 976.
60 *JAGUAR 7.0*, Schrodinger, Inc., Portland, 2007.
61 Orca, 2.6–35, F. Neese, Bonn, 2007.
62 T. Nakajima and K. Hirao, *J. Chem. Phys.*, 2002, **116**, 8270.
63 A. Schafer, C. Huber and R. Ahlrichs, *J. Chem. Phys.*, 1994, **100**, 5829.
64 E. V. Lenthe, E. J. Baerends and J. G. Snijders, *J. Chem. Phys.*, 1993, **99**, 4597.
65 M. Douglas and N. M. Kroll, *Ann. Phys.*, 1974, **82**, 89.
66 J.-J. Zhang, S.-M. Hu, S.-C. Xiang, L.-S. Wang, Y.-M. Li, H.-S. Zhang and X.-T. Wu, *J. Mol. Struct.*, 2005, **748**, 129.
67 J.-J. Zhang, S.-M. Hu, S.-C. Xiang, X.-T. Wu, L.-S. Wang and Y.-M. Li, *Polyhedron*, 2006, **25**, 1.
68 L. Maron and O. Eisenstein, *J. Phys. Chem. A.*, 2000, **104**, 7140; M. U. Kramer, D. Robert, S. Arndt, P. M. Zeimentz, T. P. Spaniol, A. Yahia, L. Maron, O. Eisenstein and J. Okuda, *Inorg. Chem.*, 2008, **47**, 9265.
69 J.-P. Costes and L. Vendier, *C. R. Chim.*, 2010, **13**, 661.
70 It is important to note here that although the magnitude of the computed J_1-J_3 are very small numbers which is at best at the limit of the theoretical level employed, we believe that the trend observed within a structure is still useful to understand the behaviour of the particular structural parameters on the *J* values.
71 M. Jung, A. Sharma, D. Hinderberger, S. Braun, U. Schatzschneider and E. Rentschler, *Eur. J. Inorg. Chem.*, 2009, 1495; A. Caneschi, A. Dei, D. Gatteschi, L. Sorace and K. Vostrikova, *Angew. Chem., Int. Ed.*, 2000, **39**, 246; C. Benelli, A. Caneschi, D. Gatteschi, L. Pardi and P. Rey, *Inorg. Chem.*, 1998, **29**, 4223.

